Eur. Phys. J. D **19**, 327–331 (2002)
DOI: 10.1140/epjd/e20020091

THE EUROPEAN PHYSICAL JOURNAL D
EDP Sciences
Società Italiana di Fisica
Springer-Verlag 2002

Sensitive detection of methane and nitrous oxide isotopomers using a continuous wave quantum cascade laser

G. Gagliardi[1,a], F. Tamassia[1,b], P. De Natale[2], C. Gmachl[3], F. Capasso[3], D.L. Sivco[3], J.N. Baillargeon[3], A.L. Hutchinson[3], and A.Y. Cho[3]

[1] European Laboratory for Non-Linear Spectroscopy and Istituto Nazionale per la Fisica della Materia, University of Firenze, largo E. Fermi 2, 50125 Firenze, Italy
[2] Istituto Nazionale di Ottica Applicata, largo E. Fermi 6, 50125 Firenze, Italy
[3] Bell Laboratories, Lucent Technologies, 600 Mountain avenue, Murray Hill, NJ 07974, USA

Received 14 March 2002

Abstract. A continuous wave quantum cascade laser (QCL), operating near 8.1 μm, was used for wavelength modulation spectroscopy of methane (CH_4) and nitrous oxide (N_2O) stable isotopes. Several rotational transitions of $^{14}N_2{}^{16}O$, $^{15}N^{14}N^{16}O$, $^{14}N_2{}^{18}O$, $^{14}N_2{}^{17}O$, $^{13}CH_4$ and $^{12}CH_4$ fundamental bands were detected. The noise-equivalent absorbance was measured to be less than 10^{-5} in a 1-Hz bandwidth. A characterization of the laser source was also performed. The use of a QCL spectrometer for high-precision isotope ratio measurements is discussed.

PACS. 42.62.Fi Laser spectroscopy – 42.55.Px Semiconductor lasers; laser diodes – 33.20.Ea Infrared spectra

1 Introduction

During the last years, infrared laser spectroscopy has been the ideal choice for a wide range of monitoring and analytical applications and, in particular, for trace gases detection with high sensitivity and selectivity [1–3]. In many cases, the possibility to retrieve quantitative and accurate information is also of crucial importance. Since most of the fundamental absorption bands of molecular species occur in the mid-infrared, lead-salt diode lasers have been commonly used as tunable sources for these purposes [4]. Nevertheless, these devices are limited in performance by their low optical power and poor spectral purity as well as by multimode operation. On the other hand, non-linear optical techniques like difference-frequency generation (DFG), which are frequently used to generate radiation from 3 to 5 μm, require more complicated set-ups [5,6]. Recently, new types of semiconductor lasers have been developed, extending their spectral coverage to longer wavelengths and keeping the advantageous tunability of conventional distributed-feedback (DFB) or distributed Bragg reflection (DBR) diode lasers as well. Quantum cascade (QC) lasers, first developed at Bell Labs in 1994 [7], are the most attractive example, covering the spectral region from 3.5 to 24 μm [8]. In a QC laser only the electrons make transitions between bound states created by quantum confinement in ultra-thin alternating layers of InGaAs or AlInAs. In this way, the emission frequency is only determined by the layer thickness, regardless of the bandgap of the constituent material. The structure of the active region relies on a cascade of identical stages (often around 20–70) which enables one electron to emit many photons. The QC lasers can be operated in pulsed mode, at room temperature, or in continuous wave (cw) at cryogenic temperatures, generating output powers up to 200 mW. Quite recently, a new QC device, able to operate cw up to 246 K, has been developed [9].

The spectral window between 3 and 8 μm is particularly important for several atmospheric species, such as methane, nitrous oxide, ammonia, carbon dioxide and water vapor. Quite recently, it has been demonstrated that QC-laser-based spectrometers can be successfully used for absorption spectroscopy on IR transitions not accessible to room-temperature diode lasers [8–11]. This advantage can be exploited for low concentration gas measurement as well as for determination of the isotopic content of a given species with high precision and accuracy. Isotopic analysis is particularly relevant for investigation of environmental processes and for biomedical and geophysical applications as it can provide information not attainable through gas concentration measurements alone [12,13]. However, accuracy and precision in the order of 10^{-3} are required for

[a] *On leave from*: Dipartimento di Scienze Ambientali, Seconda Università di Napoli, via Vivaldi 43, 81100 Caserta, Italy. e-mail: gagliardi@na.infn.it
[b] *Current address*: Dipartimento di Chimica Fisica e Inorganica, Università di Bologna, viale Risorgimento 4, 40136 Bologna, Italy.

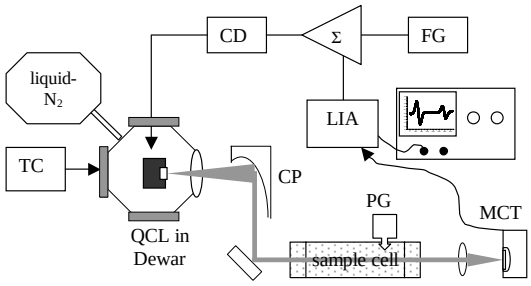

Fig. 1. Sketch of the experimental apparatus. QCL = quantum cascade laser; CP = collimation parabola; MCT = HgCdTe detector; FG = function generator; LIA = Lock-in amplifier; CD = current driver; TC = temperature controller; PG = pressure gauge.

such studies. For this purpose, stable isotopes analysis is usually carried out by means of sensitive mass spectrometers, with accuracy and precision of 0.03 . Nevertheless, mass spectrometers are expensive and sophisticated instruments that present some limitation in some cases of practical interest. First of all, different isotopomers may overlap in mass. This is, for instance, the case of $^{12}CH_3D$ and $^{13}CH_4$, or $^{15}N^{14}N^{16}O$ and $^{14}N^{15}N^{16}O$. Moreover, in the case of condensable gases, this approach is associated with a time-consuming sample pre-treatment that may severely limit the achievable accuracy. Such limitations explain the growing interest towards alternative methods, like laser absorption spectroscopy, which is based on the isotopic shift of molecular ro-vibrational lines. Indeed, using a cw tunable laser source, the spectral features of different isotopic molecular species can be easily detected in a single frequency scan [14–16]. Simultaneous recording of the signals coming from two different absorption cells, one for the sample gas and another one containing a mixture of known isotopic composition, enables one to measure the isotope ratio of the sample with respect to the standard.

In this paper, a liquid-N_2-cooled QC laser, operating around 1 240 cm^{-1}, is used for sensitive detection of methane and nitrous oxide isotopomers, by means of wavelength modulation absorption spectroscopy (WMS). Wavelength calibration and characterization of the laser emission were performed through direct observations of absorption spectra. The possibility to measure CH_4 and N_2O isotope ratios is examined. The main factors influencing reproducibility and accuracy in isotopic measurements are considered.

2 Description of the spectrometer

Figure 1 shows the experimental arrangement. A QC-DFB laser, emitting 50 mW cw around 1 240 cm^{-1}, was mounted in a liquid-N_2 Dewar (Janis mod. ST-100). The laser temperature, ranging from 80 to 87 K, was actively stabilized by means of a PID controller (LakeShore mod. 330). A homemade low-noise high-current source, driven by an external waveform generator, provided the laser current. The laser frequency was scanned by a triangular current ramp with a frequency of about 100 Hz. The strongly diverging QC laser radiation was first collected by a ZnSe AR-coated lens, with a 150-mm focal length and a 25.4-mm diameter, and then reduced to a quasi-collimated beam using an off-axis parabolic mirror with an effective focal length of 191 mm. The laser beam was directed to a 17-cm-long sample-gas cell, equipped with KBr windows. The pressure was monitored by a 10-torr full-scale capacitance gauge (Varian mod. VCMT11). The transmitted radiation was focused onto a liquid-N_2-cooled photoconductive HgCdTe detector by a 50-mm ZnSe lens. The detector signal was then amplified by a 0.1 Hz–1 MHz preamplifier.

In order to increase the sensitivity of the spectrometer, wavelength modulation spectroscopy (WMS), with 1st harmonic detection, was also performed. The QC laser frequency was modulated adding a 10-kHz sinusoidal signal to the injection current, with a modulation index varying from 1.3 to 1.7, while the laser frequency was scanned across an absorption line using a triangular wave at a typical frequency of 2.5 Hz. Phase sensitive detection, at the modulation frequency, was provided by a lock-in amplifier and the demodulated signal was sent to a 500-MHz digital oscilloscope for data acquisition. A total number of 10 000 points were acquired for each spectrum. The effective detection bandwidth was about 4 Hz, taking into account the lock- in time constant as well as spectra averaging.

3 Characterization of the quantum cascade laser source

Quantum cascade lasers are expected to exhibit excellent performance in terms of frequency stability and spectral purity. Actually, the line-width of a conventional diode laser is usually degraded, with respect to the Schawlow-Townes limit, because of the so-called "alpha parameter" (α), which takes into account the refractive index variations due to population inversion fluctuations [17]. Thanks to the different nature of the optical transition, quantum cascade lasers are expected to have a α value close to zero. As a consequence, the intrinsic laser line-width of a QC device should be significantly smaller than that of an interband diode laser. In a recent experiment, the spectral width of a QC laser, emitting around 5.2 μm, has been investigated in a heterodyne detection scheme [18]. In that paper, linewidths smaller than 1 MHz were measured and a strong dependence on the current supply performance was observed. Furthermore, in another experiment the frequency of an 8.5-μm QC-DFB laser was stabilized to the side of a molecular resonance, by means of an electronic feedback loop, yielding a laser line-width of 12 kHz [19]. An analysis of both spectral and spatial features of our QC laser was performed in view of the possible use in conjunction with high-finesse cavities or multiple-reflections cells. In Figure 2 the absorption spectrum recorded at a very low methane pressure in the sample cell is shown. The transition was identified as the P(10) A2(1)–A1(1) belonging to

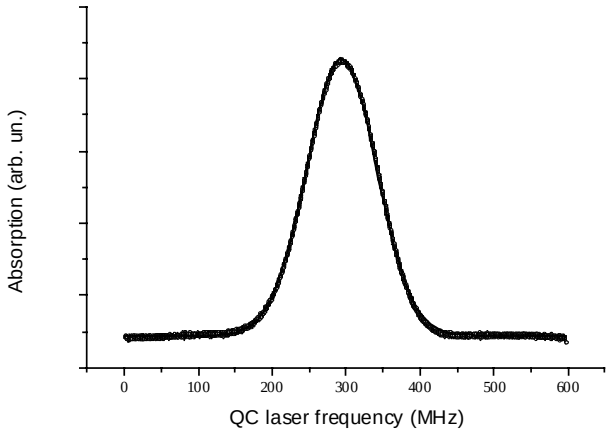

Fig. 2. Spectroscopic estimation of the laser line-width. $^{12}CH_4$ sample pressure: 30 mtorr. The experimental curve (solid circles) is fitted to a Voigt function (continuous line), yielding a Lorentzian contribution of about 3 MHz.

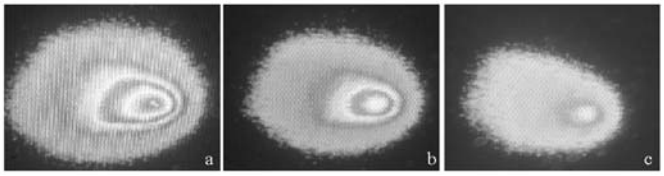

Fig. 3. Spatial distribution of the QC laser intensity, recorded with a thermal camera, for an incident power of (a) 47 mW, (b) 32 mW, (c) 15 mW. The orientation of the laser plane is vertical.

the ν_4 vibrational band [20]. By fitting the line-shape to a Voigt profile, it was possible to extrapolate a homogeneous contribution to the line-width equal to 3.5 ± 0.2 MHz in a 1-ms time scale. It represents an estimation of the upper limit to the free-running laser line-width if its power spectrum is supposed to be Lorentzian, that is, its frequency noise is dominated by "white" noise. This value is considerably lower than those found in previous spectroscopic investigations [11,16] and already gives a clear indication of the excellent spectral characteristics of QC lasers. Anyway, our value is slightly higher than that reported in [18]; additional frequency fluctuations may be addressed to laser driver current noise, although a thorough investigation of QC laser phase noise is beyond the aim of the present work.

The beam quality of the QC laser was also examined. In Figure 3, three pictures of the laser spatial mode are shown as observed by a thermal imaging system (Inframetrics mod. 600) after the collimating optics, for different values of the incident power, exhibiting no appreciable change in the beam shape. The infrared spot appears elliptic and astigmatic, as expected for a diode laser source, as well as affected by coma mainly due to the off-axis parabola used for collimation.

Several pairs of absorption lines of CH_3I, already assigned on the basis of a Fourier Transform Infrared (FTIR) spectrum, were used as a reference in order to retrieve the relationship between laser current and frequency. The

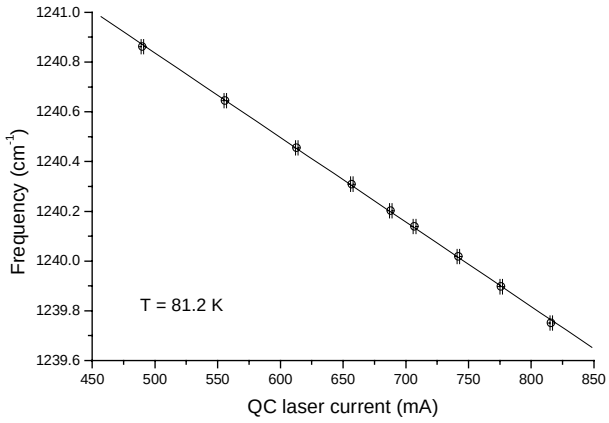

Fig. 4. QC laser frequency as a function of the injection current at $T = 81.2$ K.

result is well approximated by a linear dependence with a slope of 102 ± 1 MHz/mA as shown in Figure 4. The wavelength tunability *vs.* temperature was found to be about 2.2 GHz/K. Continuous frequency scans, as wide as 1 GHz, were possible without mode jumps in the whole operating temperature range ($80 \div 87$ K). In principle, the laser can be operated up to about 100 K although a strong reduction of the emitted power would occur.

4 Heterodyne detection of N_2O and CH_4 isotopomers

Several physical and chemical phenomena, such as evaporation and oxidation, discriminate among different isotopomers. This so-called fractionation is often typical of the processes involved and can be exploited to achieve a deeper understanding of the processes themselves. For this reason, rare isotopes act as perfect natural tracers for a large number of studies in animal behavior, food product authenticity, paleoclimatology and global warming. For instance, the $^{13}CH_4/^{12}CH_4$ and $^{12}CH_3D/^{12}CH_4$ isotope ratios in atmosphere give information on the relative contributions of the various sources to the global methane budget, including its different production pathways [22,23].

In our experiment, detection of $^{12}CH_4$, $^{13}CH_4$, $^{14}N_2{}^{16}O$, $^{15}N^{14}N^{16}O$, $^{14}N_2{}^{18}O$ and $^{14}N_2{}^{17}O$ molecules in natural isotopic abundance for CH_4 and N_2O pure samples was demonstrated using wavelength modulation spectroscopy, with first harmonic detection. In the spectral window covered by the QC laser, from 1 239.5 to 1 241.0 cm^{-1}, CH_4 and N_2O exhibit strong transitions belonging to their fundamental vibrations, with absorption coefficient of about 7×10^{-1} and 3×10^{-2} $cm^{-1}\,torr^{-1}$, respectively. In that region, an overlap between the P branch of the $2\nu_4$–ν_4 hot band of $^{12}CH_4$ and the P branch of the ν_4 bending mode of $^{13}CH_4$ takes place, thus making possible a partial compensation of the difference in their natural abundance (98.8% and 1.1% respectively). The observed spectrum corresponding to the lines P(7) A1(2)–A2(1) of

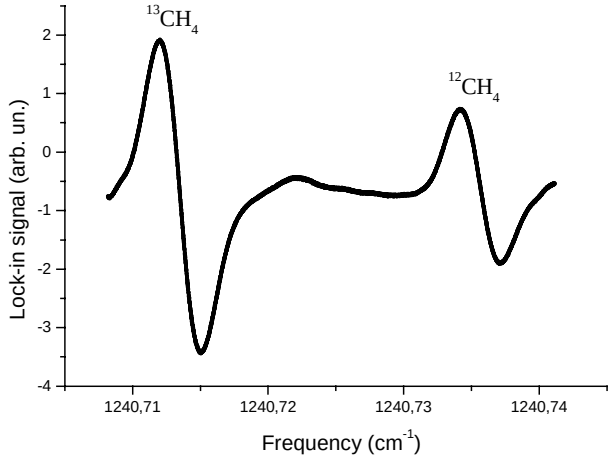

Fig. 5. First harmonic simultaneous detection of lines P(10) A2(1)–A1(1) of $^{13}CH_4$ ν_4 band, at 1 240.714 cm^{-1}, and P(7) A2(1)–A1(2) of $^{12}CH_4$ $2\nu_4-\nu_4$, at 1 240.736 cm^{-1}. The methane total pressure is 150 mtorr.

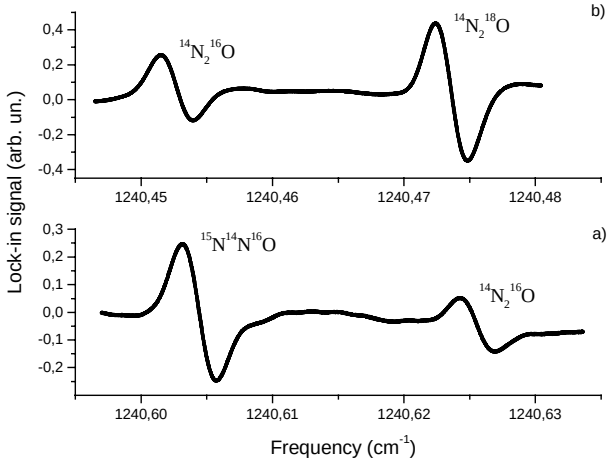

Fig. 6. (a) First harmonic phase-sensitive detection of lines P(34) of the $^{15}N^{14}N^{16}O$ 00^01–00^00 band and P(42) of the $^{14}N_2{}^{16}O$ 00^02–00^01 band, recorded with 80 mtorr of N_2O in natural abundance. (b) First harmonic signals corresponding to lines P(55) of the $^{14}N_2{}^{16}O$ 01^11–$01^{1e}0$ band and P(8) of the $^{14}N_2{}^{18}O$ 00^01–00^00 band (N_2O pressure = 80 mtorr).

the $^{12}CH_4$ $2\nu_4$–ν_4 band and P(10) A1(1)–A2(1) of the $^{13}CH_4$ ν_4 band [21] is shown in Figure 5. It was obtained in the presence of 150 mtorr of pure methane in natural abundance, with a 1-ms integration time and signal averaging over 30 scans. The signal-to-noise ratio is very high, although some small absorption lines, probably due to ambient water vapor, also emerge from the noise floor. From recordings like this, a minimum detectable absorption of less than one part in 10^5 can be estimated in a 1-Hz detection bandwidth. This value corresponds to a minimum CH_4 pressure of about 3 μtorr in a 1-m-long path.

A similar situation occurs for N_2O, as the center of the $^{14}N_2{}^{16}O$ 00^01–00^00 fundamental band lies in a different spectral region, near 1 271 cm^{-1}, with respect to its isotopomers. The lines P(34) of the $^{15}N^{14}N^{16}O$ 00^01–00^00 band and P(42) of the $^{14}N_2{}^{16}O$ 00^02–00^01 band, P(55) of the $^{14}N_2{}^{16}O$ 01^11–$01^{1e}0$ band and P(8) of the $^{14}N_2{}^{18}O$ 00^01–00^00 band [24] are shown in Figures 6a and 6b respectively. They were both recorded at a pressure of 80 mtorr of nitrous oxide in natural abundance. The main limitation to the achievable sensitivity is the presence of strong $N_2{}^{16}O$ absorption lines in the neighborhood as well as interference fringes due to reflections from uncoated optical elements (see Fig. 6a).

The possibility to perform isotope ratio measurements on these molecular species has been examined. A test evaluation of the experimental reproducibility was performed through a set of 40 acquisitions of isotopic spectra, with identical experimental conditions, for a 2 600-s total measurement time. We found a standard deviation of the ratio between the peak-to-peak signals, corresponding to $^{12}CH_4$ and $^{13}CH_4$ line pair, of a few for $P = 150$ mtorr and 17-cm pathlength. Admittedly, the obtained precision is still poor if compared to that given in recent works with diode lasers around 1.66 μm [14]. For example, in reference [14], the achieved precision is 0.3 that is considerably better than our result. Nevertheless, if our results are scaled to the same experimental conditions, namely 100-m path length and 0.5 torr pressure, a level of precision within 0.01 can be expected with our spectrometer. Indeed, the main advantage of QCLs for spectroscopic applications are their wide tunability and high spectral purity in a spectral range where the strongest ro-vibrational transitions lie. For the absorption lines we considered, the intensity is at least a factor 100 higher than a typical transition in the near-infrared. Furthermore, the achievable reproducibility in our experiment is partially limited by a non-flat background in the recorded signals due to the residual amplitude modulation. Of course, further baseline flattening can be obtained by third or higher-order harmonic detection.

The ratio $^{13}C/^{12}C$ is usually determined relative to the standard (Vienna Pee Dee Belemnite) and expressed in the following notation

$$\delta^{13}C = \left(\frac{R^{13}_{\text{sample}}}{R^{13}_{\text{standard}}} - 1 \right) \times 1\,000, \qquad (1)$$

being R^{13} the ratios $^{13}CH_4/^{12}CH_4$ in the sample and the standard. Analogously, the $^{18}O/^{16}O$ and $^{17}O/^{16}O$ isotope ratios in N_2O, can be defined with respect to the international Vienna Standard Mean Ocean Water (VSMOW). The abundance ratios are determined by comparing the ratio of the absorbances of two selected isotopic lines between the sample gas and a standard gas. This procedure can be accomplished using two identical cells, kept at the same temperature within a given interval ΔT. This is the main factor influencing the accuracy in isotope ratio measurements. The order of magnitude of ΔT depends on the temperature sensitivity of the ratio of the two line-strengths. Hence, the choice of appropriate molecular transitions is of crucial importance in isotopic measurements for a given species using laser absorption spectroscopy. For the line pairs of Figures 5 and 6, we have

calculated a temperature dependence of the intensity ratios of 1.5%/K and 2.5%/K respectively. This calculation was carried out using the following expression, for $T_0 = 300$ K:

$$S(T_0) = S(T)\frac{Q_{\rm vib}(T)}{Q_{\rm vib}(T_0)}\frac{Q_{\rm rot}(T)}{Q_{\rm rot}(T_0)}\exp\left[\frac{E''hc}{k_{\rm B}}\left(\frac{T_0 - T}{T_0 T}\right)\right], \quad (2)$$

where $S(T_0)$ is the line-strength at a reference temperature T_0, E'' is the lower-state energy of the transition and $Q(T)$ the partition function. For a linear molecule, like N_2O, the above equation simplifies to

$$S(T_0) = S(T)\frac{T}{T_0}\exp\left[\frac{E''hc}{k_{\rm B}}\left(\frac{T_0 - T}{T_0 T}\right)\right]. \quad (3)$$

This means the effect of temperature changes can be significantly reduced by choosing transitions having nearly the same lower-state energy. For CH_4 isotopomers, ΔT should be as small as 0.1 K in order to achieve an accuracy of 1 , at the wavelength we are now operating. Moving towards longer wavelengths, a more favorable temperature dependence can be found for CH_4. In the spectral region near 1 240.9 cm^{-1}, some closely located lines, such as P(10) E(1)–E(1) for $^{13}CH_4$ and Q(12) F1(2)–F2(2) for $^{12}CH_4$, have interesting features. In this case an accuracy of 0.4 could be obtained for the sample and the standard gases assuming a temperature stability of 0.1 K. Nevertheless, all these lines are at least a factor 10 weaker than the selected transitions, and the use of a multipass cell would be necessary. For the N_2O isotopomers, the situation is different. A more favorable set of lines can be found for $\delta^{14}N$ and $\delta^{18}O$ measurements, but most of them are out of our QC laser spectral coverage.

5 Conclusions

A continuous-wave quantum cascade laser-based spectrometer, operating near 8.06 μm, was developed for sensitive spectroscopy of methane and nitrous oxide isotopomers. Using wavelength modulation spectroscopy, with first harmonic detection, we found the spectrometer sensitivity to be better than 1×10^{-5} $Hz^{-1/2}$, corresponding to a minimum pressure of 1 and 3 μtorr m for methane and nitrous oxide, respectively. We carried out a characterization of the QC laser spectral and spatial properties in view of its application to saturated-absorption spectroscopy as well as for efficient coupling to high-finesse cavities. Images of the QC laser mode were recorded and an estimate of the QC laser line-width was performed through direct observation of absorption spectra, yielding approximately 3 MHz. Furthermore, we analyzed the feasibility of isotopic composition analysis for different isotopomers of CH_4 and N_2O, in natural abundance samples. A reproducibility of a few in detection of $^{13}CH_4$ and $^{15}N^{14}N^{16}O$, $^{14}N_2{}^{18}O$, $^{14}N_2{}^{17}O$ isotopic species was evaluated for low-pressure pure samples. However, this value can be improved by at least two orders of magnitude using longer absorption path lengths. In addition, we estimated the level of achievable accuracy, in our spectral region. For this purpose, the temperature sensitivity of the considered transitions was investigated in view of possible $\delta^{13}C$, $\delta^{18}O$ and $\delta^{15}N$ measurements.

The authors wish to thank Massimo Inguscio and Gianfranco Di Lonardo for helpful and stimulating discussions. The work performed at Bell Laboratories, Lucent Technologies was partly supported by Darpa/US Army Research Office under contract DAAD19-00-C-0096.

References

1. L. Gianfrani, G. Gagliardi, G. Pesce, A. Sasso, Appl. Phys. B **64**, 487 (1997).
2. P. Werle, R. Mucke, F. D'Amato, T. Lancia, Appl. Phys. B **67**, 307 (1998).
3. L. Gianfrani, P. De Natale, G. De Natale, Appl. Phys. B **70**, 467 (2000).
4. P. Werle, Spectrochim. Acta A **54**, 197 (1998).
5. D. Mazzotti, P. De Natale, G. Giusfredi, C. Fort, J.A. Mitchell, L. Hollberg, Appl. Phys. B **70**, 747 (2000).
6. K.P. Petrov, L. Goldberg, W.K. Burns, R.F. Curl, F.K. Tittel, Opt. Lett. **21**, 86 (1996).
7. J. Faist, F. Capasso, D.L. Sivco, C. Sirtori, A.L. Hutchinson, A.Y. Cho, Science **264**, 553 (1994).
8. F. Capasso *et al.*, IEEE J. Quant. Electron. **6**, 931 (2000), and references therein.
9. D. Hofstetter *et al.*, Appl. Phys. Lett. **78**, 1964 (2001).
10. C.R. Webster *et al.*, Appl. Opt. **40**, 321 (2001).
11. S.W. Sharpe *et al.*, Opt. Lett. **23**, 1396 (1998).
12. C.D. Keeling, T.P. Whorf, M. Wahlen, J. van der Plicht, Nature **375**, 666 (1995).
13. D. Tedesco, P. Scarsi, Earth Plan. Sci. Lett. **171**, 465 (1999).
14. K. Uehara *et al.*, Sens. Act. B **74**, 173 (2001).
15. E.R.Th. Kerstel *et al.*, Anal. Chem. **71**, 5297 (1999).
16. A.A. Kosterev *et al.*, Opt. Lett. **24**, 1762 (1999).
17. C.H. Henry, IEEE J. Quant. Electr. **18**, 259 (1982).
18. H. Ganser *et al.*, Opt. Commun. **197**, 127 (2001).
19. R.M. Williams *et al.*, Opt. Lett. **24**, 1844 (1999).
20. A.G. Robiette, J. Mol. Spectrosc. **86**, 143 (1981).
21. A. Chedin, N. Husson, N.A. Scott, D. Gautier, J. Mol. Spectrosc. **71**, 343 (1978).
22. S.C. Tyler, IGAC Newslett. **16**, 3 (1999).
23. P. Bergamaschi, M. Schupp, G.W. Harris, Appl. Opt. **33**, 7704 (1994).
24. L.S. Rothmann *et al.*, J. Quant. Spec. Rad. Transf. **60**, 665 (1998).